

# Multiple Functions for Actin during Filamentous Growth of *Saccharomyces cerevisiae*<sup>V</sup>

Brian M. Cali,\* Timothy C. Doyle,<sup>†‡</sup> David Botstein,<sup>†</sup> and Gerald R. Fink<sup>\*§||</sup>

\*Whitehead Institute for Biomedical Research and <sup>§</sup>Department of Biology, Massachusetts Institute of Technology, Cambridge, Massachusetts 02142; and <sup>†</sup>Department of Genetics, Stanford University Medical Center, Stanford, California 94305

Submitted January 16, 1998; Accepted March 13, 1998  
Monitoring Editor: David Drubin

*Saccharomyces cerevisiae* is dimorphic and switches from a yeast form to a pseudohyphal (PH) form when starved for nitrogen. PH cells are elongated, bud in a unipolar manner, and invade the agar substrate. We assessed the requirements for actin in mediating the dramatic morphogenetic events that accompany the transition to PH growth. Twelve “alanine scan” alleles of the single yeast actin gene (*ACT1*) were tested for effects on filamentation, unipolar budding, agar invasion, and cell elongation. Some *act1* mutations affect all phenotypes, whereas others affect only one or two aspects of PH growth. Tests of intragenic complementation among specific *act1* mutations support the phenotypic evidence for multiple actin functions in filamentous growth. We present evidence that interaction between actin and the actin-binding protein fimbrin is important for PH growth and suggest that association of different actin-binding proteins with actin mediates the multiple functions of actin in filamentous growth. Furthermore, characterization of cytoskeletal structure in wild type and *act1/act1* mutants indicates that PH cell morphogenesis requires the maintenance of a highly polarized actin cytoskeleton. Collectively, this work demonstrates that actin plays a central role in fungal dimorphism.

## INTRODUCTION

Genetic and biochemical studies in the budding yeast *Saccharomyces cerevisiae* have provided important insights into the cellular functions of actin and actin-binding proteins. More than 80 sequenced mutations affecting the single yeast actin gene (*ACT1*) have been identified (Ayscough and Drubin, 1996). Collectively, these mutations affect many aspects of cell growth, including secretion (Novick and Botstein, 1985), endocytosis (Riezman *et al.*, 1996), bipolar bud site selection (Yang *et al.*, 1997), and organellar trafficking (Drubin *et al.*, 1993; Simon *et al.*, 1995). Numerous yeast actin-binding proteins have also been identified using genetic, biochemical, and two-hybrid approaches. Mutations in genes encoding many such proteins perturb actin cytoskeletal structure and/or function (for exam-

ples and reviews, see Drubin *et al.*, 1988, 1990; Adams and Botstein, 1989; Adams *et al.*, 1989; Liu and Bretscher, 1989; Amatruda *et al.*, 1990; Welch *et al.*, 1994; Amberg *et al.*, 1995, 1997; Brower *et al.*, 1995; Ayscough and Drubin, 1996; Riezman *et al.*, 1996; Botstein *et al.*, 1997).

Most observations regarding the yeast actin cytoskeleton have been made on yeast form (YF)<sup>1</sup> cells grown in the presence of ample nutrients. Under these conditions, diploid *S. cerevisiae* grow by budding to produce oval-shaped daughters that separate from the mother cell at cytokinesis and remain on the surface of the agar substrate. However, *S. cerevisiae* is dimorphic. When starved for nitrogen in the presence of a fermentable carbon source, *S. cerevisiae* switches to a pseudohyphal (PH), or filamentous, mode of growth (Gimeno *et al.*, 1992). PH cells are much longer and thinner than YF cells, remain attached to mothers after

<sup>||</sup> Corresponding author. E-mail address: fink@wi.mit.edu.

<sup>‡</sup> Present address: Molecular Biology Institute, Department of Chemistry and Biochemistry, UCLA, Los Angeles CA 90095.

<sup>V</sup> Online version of this article contains video material for Figures 6 and 7. Online version available at [www.molbiolcell.org](http://www.molbiolcell.org).

<sup>1</sup> Abbreviations used: GFP, green fluorescent protein; PH, pseudohyphal; SLAD, synthetic low-ammonia dextrose; YF, yeast form.

cytokinesis, and invade the agar substrate. These growth characteristics, coupled with a unipolar budding pattern, with daughters predominantly budding away from mothers, lead to growth of filaments of long cells away from the body of the colony.

Differences in the polarity of the actin cytoskeleton between YF and PH cells suggest a specialized role for the actin cytoskeleton in PH growth. The yeast actin cytoskeleton comprises two major structures, patches and cables. Actin patches are punctate "dots" of filamentous actin present at the cell cortex, whereas cables are oriented along the mother–bud axis and have been described as cytoplasmic (Adams and Pringle, 1984). Patches are highly mobile (Doyle and Botstein, 1996; Waddle *et al.*, 1996) and are localized to areas of new cell growth throughout the cell cycle. In PH cells, actin patches are polarized to the distal tip of the daughter cell throughout bud growth and then repolarize to the site of septation shortly before cytokinesis (Kron *et al.*, 1994). This behavior contrasts with that of patches in YF cells, where there is a distinct period between bud emergence and cytokinesis when patches are distributed around the entire cortex of the emerging bud (the isotropic growth phase) (Lew and Reed, 1993). These differences indicate that actin cytoskeletal structure and dynamics are regulated differently in YF and PH cells.

Genetic analysis also indicates that the actin cytoskeleton has an important function in PH growth. In a general screen for mutants defective for filamentation, Mösch and Fink (1997) identified mutations in several genes encoding cytoskeletal proteins. These include the genes encoding the actin-binding proteins Tpm1p (tropomyosin), Srv2p (cyclase-associated protein), and the formin homology domain protein Bni1p. Deletion of *SLA2*, which encodes a protein with homology to the focal adhesion protein talin, was also shown to block filamentation (Yang *et al.*, 1997).

Here we have investigated the functional requirements for actin in mediating the dramatic changes in agar invasion, bud site selection pattern, and cell shape that accompany the transition from growth in the YF to PH growth. This work indicates that actin has multiple functions in filamentous growth and provides new insight into actin structure–function relationships. In addition, image analysis of wild type and *act1/act1* mutants suggests an important role for cortical actin patch polarization in the morphogenesis of the PH cell.

## MATERIALS AND METHODS

### *Yeast Strains, Plasmids, and Microbiological Methods*

Yeast strains used in this study are isogenic and derived from the  $\Sigma$ 1278b strain background (Table 1). Standard media and methods of sporulation, tetrad dissection, and scoring of mating type were as previously described (Guthrie and Fink, 1991). Synthetic low-am-

monia dextrose (SLAD) medium has also been described (Gimeno *et al.*, 1992). Plasmids used in this study have been previously described: pIL30 (Laloux *et al.*, 1994), pRS314 and pRS316 (Sikorski and Hieter, 1989), and AAB117 and AAB289 (Brower *et al.*, 1995). Transformation was performed by the lithium acetate transformation method (Ito *et al.*, 1983; Gietz *et al.*, 1992).

### *Genetic Manipulations and Strain Constructions*

Actin mutant strains were constructed by single-step gene replacement using donor DNA fragments containing the desired *act1* allele with *HIS3* integrated just downstream of the *act1* coding sequence (*act1-x::HIS3*) and an *act1 $\Delta$ ::LEU2/ACT1* heterozygous diploid as recipient. To generate the *act1 $\Delta$ ::LEU2/ACT1* heterozygote for eventual gene replacement, an *ACT1* disruption construct was made by first subcloning the 3.8-kb *EcoRI* fragment containing *ACT1* from pKFW29 (Wertman *et al.*, 1992) into the *EcoRI* site of pUC19 to generate BCB109. BCB109 was digested with *BclI* and *XhoI* and ligated in the presence of an *XhoI*–*BglIII* fragment from YEp13 that contains *LEU2*. The resultant *act1 $\Delta$ ::LEU2* construct in pUC19 (BCB207) deletes all but the first three amino acids of the *ACT1* coding region and contains 1246 bp upstream and 1118 bp downstream of *ACT1*. BCY116 was transformed with the *ApaI*–*SmaI* fragment of BCB207, and Leu<sup>+</sup> transformants were identified. Genomic DNA from 27 Leu<sup>+</sup> transformants was tested by PCR for linkage of a *LEU2*-specific oligonucleotide (LEU2-P3: 5'-GATTTCITGACCA-ACGTGGTC) with an oligonucleotide (ACT1-8: 5'-TTCAAACCTGCTGTGATCGG) specific to a genomic region just outside that contained in BCB207 and oriented toward LEU2-P3. Twelve transformants gave the 2.0-kb product expected for a disruptant. Three of these putative heterozygotes segregated two viable Leu<sup>-</sup>:2 lethal spores, confirming heterozygosity for *act1 $\Delta$ ::LEU2*. One such heterozygote was kept as BCY144.

To introduce the *act1* alleles by gene replacement, BCY144 was transformed independently with each of the *EcoRI*-digested plasmid derivatives of pKFW46 carrying the relevant *act1* alleles with *HIS3* integrated downstream (Wertman *et al.*, 1992). His<sup>+</sup> transformants were selected and screened for those that were Leu<sup>-</sup>. Two independent His<sup>+</sup> Leu<sup>-</sup> transformants were retained as candidate *act1-x::HIS3/ACT1* heterozygotes, where *x* represents any given *act1* allele. As *HIS3* is tightly linked to each of these alleles, they can be followed in crosses by monitoring histidine prototrophy. Heterozygotes for each of the alleles were sporulated, and the tetrads were dissected. Nine alleles were viable as haploids at 30°C. Strains heterozygous for three of the alleles (*act1-109*, *act1-110*, and *act1-131*) segregated two viable His<sup>-</sup>:2 lethal spores, indicating that these *act1* alleles are recessive lethal in  $\Sigma$ 1278b, as they are in S288c (Wertman *et al.*, 1992). Presence of the desired *act1* mutation was confirmed by restriction analysis of an *act1* PCR product amplified from the genome. This assignment was possible because each of the *act1* alleles analyzed in this study creates or destroys a restriction site in *ACT1* (Wertman *et al.*, 1992). To confirm the presence of the *act1* mutation in each of these strains, *act1* was amplified by PCR with *Taq* polymerase using oligonucleotides *act1-4* (5'-CTTTCC-TTAAAAATACTTTATTA) and *ACT1-10* (5'-GTACTAACATCGA-TTGCTTC) under standard conditions. The expected 1275-bp product was digested with enzymes diagnostic for each mutation as previously described (Wertman *et al.*, 1992). Restriction fragments of the size expected for the appropriate allele were seen in all cases. For all viable alleles, *act1* was amplified from two independent His<sup>+</sup> haploids segregated from the original heterozygous diploids. For the recessive lethal alleles *act1-109*, *act1-110*, and *act1-131*, the *ACT1* alleles were amplified from the heterozygous diploid, and both wild-type and mutant restriction patterns were observed.

*act1/act1* homozygotes were constructed by first transforming *act1-x::HIS3/ACT1* heterozygous diploids to Leu<sup>+</sup> with the *LEU2* *CEN* plasmid pIL30 (Laloux *et al.*, 1994). Sporulation, dissection, and mating of appropriate haploids were then used to generate prototrophic diploids homozygous for each of the viable *act1* alleles

(Table 1). For analysis of the recessive lethal alleles, the original *act1-x::HIS3/ACT1* heterozygotes were transformed to Leu<sup>+</sup> with pIL30 and used for subsequent analysis.

To generate a *sac6Δ::LEU2/sac6Δ::LEU2* diploid, a 2.9-kb genomic fragment carrying the *sac6Δ::LEU2* allele of AAY1047 (Adams *et al.*, 1995) was generated by PCR with oligonucleotides SAC6-1 (5'-GCAGTAAAGGTGCTTTGTC) and SAC6-2 (5'-AAAAGTTCA-CAGGATATATGG) and used to transform BCY333 to Leu<sup>+</sup>. Candidate *sac6Δ::LEU2/SAC6* heterozygotes were tested by PCR to identify linkage of oligonucleotides LEU2-P3 and SAC6-3 (5'-GCT-CAAGGACGCCCCATTG); one transformant that gave the appropriate product was sporulated and dissected; *sac6Δ::LEU2* was confirmed to segregate 2:2. Mating of appropriate haploids from this dissection and subsequent transformation with pRS316 generated the *sac6Δ::LEU2/sac6Δ::LEU2* homozygote BCY372.

### Assessment of Filamentation, Cell Elongation, and Invasion Phenotypes

Strains to be analyzed were streaked for well-isolated single colonies on SLAD plates, with no more than four strains per plate. Plates were incubated for 4 d at 30°C, and well-isolated colonies were scored for filamentation. Strains with no filaments extending beyond the perimeter of the colony were scored as (-) for filamentation; those with 1–10% of colonies showing some filaments were scored as (+). (++) indicates that 80–100% of colonies had filaments, yet these filaments were disorganized relative to wild type. (+++) = wild-type filamentation.

Cell elongation was quantified by growing colonies as above, scraping cells from the agar with a toothpick into 10 μl of water, and scoring morphology on a hemacytometer. Cells with length/width ratios ≥2 were scored as long cells.

To score invasion, the same plates used to score filamentation and cell elongation were washed with a stream of water. Noninvasive cells were removed by gently rubbing the agar surface. Those strains with <10% of washed colonies having residual cells in the agar, and only in the center of the colony, were scored as (-). (+) denotes strains with 10–50% of washed colonies having residual cells. Typically, only cells in the center of the colony had invaded in this class. Mutants that showed 50–100% of colonies with invaded cells were scored either as (++) or (+++) depending on whether part (++) or all (+++) of the colony diameter contained invaded cells.

### Preparation of PH Cells for Rhodamine–Phalloidin and Calcofluor Staining

Strains to be assayed were grown overnight at 30°C in 5 ml of YNB. Cells were washed once in 5 ml of water, spread on the surface of a 10.5-cm SLAD plate, and incubated 24–48 h at 30°C. For rhodamine–phalloidin staining studies, prestarved cells were collected in water and serially diluted in 1.25% alginate (wt/vol) (Sigma, St. Louis, MO; catalog number A-2158) in water. Suspensions of cells (0.5 ml) were spread thinly over the surface of a SLAD agar plate, alginate was allowed to solidify, and plates were incubated 48 h at 30°C. For fixation, alginate was removed with forceps from plates with well-separated single colonies and placed in 6 ml of 0.8 M EGTA/3.7% formaldehyde in a 15-ml polypropylene tube (chelation of calcium by EGTA causes alginate to liquefy). After 1 h with intermittent shaking, cells were washed three times in 1× PBS. Rhodamine–phalloidin staining was performed as described previously (Kron *et al.*, 1994). For calcofluor staining, prestarved cells were grown in SLAD liquid overlay media, fixed, and stained as previously described (Kron *et al.*, 1994).

### Microscopic Methods

Cells fixed and stained as above were mounted in 90% glycerol/1× PBS and viewed using epifluorescence on a Nikon (Garden City, NY) E6 inverted microscope, controlled by the Applied Precision

(Issaquah, WA) DeltaVision wide-field microscope system. Fluorescent images were obtained at 100× magnification (numerical aperture, 1.4) and captured with a Princeton Instruments (Trenton, NJ) cooled charged-couple device camera. Stacks of rhodamine and DAPI fluorescence images were captured at 0.2-μm intervals in the z-plane (1- to 3-s image capture time), and out-of-focus fluorescence was removed by iterative deconvolution (Agard *et al.*, 1989; Scalettar *et al.*, 1996). Three-dimensional representations of these two-dimensional stacks were then generated, and rotated views through the stack were obtained and used to generate stereo images.

## RESULTS

To determine the functional requirements for actin during PH growth, we have taken advantage of an extant set of “charged-to-alanine scan” alleles of *ACT1* (Wertman *et al.*, 1992). These mutations provide a number of distinct advantages for dissecting the roles of actin in PH growth. First, the residues affected by these mutations are known and can be mapped to the crystal structure of actin. Collectively these mutations affect a large portion of the solvent-exposed surface of the actin monomer. Second, the effects of these mutations on a number of actin-dependent processes have been well documented (for examples, see Read *et al.*, 1992; Drubin *et al.*, 1993; Smith *et al.*, 1995). Third, the effects of these alanine scan alleles on the binding of many actin-interacting proteins have been determined (Holtzman *et al.*, 1994; Honts *et al.*, 1994; Amberg *et al.*, 1995, 1997). This detailed information on the functions affected by these alleles provides an invaluable guide in assessing the possible roles of actin and actin-binding proteins in PH growth.

### Actin Mutants Exhibit Filamentation Defects

Twelve alanine scan *act1* alleles were introduced into a strain (a Σ1278b derivative) capable of PH growth (Gimeno *et al.*, 1992) (see MATERIALS AND METHODS for details). These constructions were necessary because the *act1* alleles were originally studied in S288c (Wertman *et al.*, 1992), a background that does not exhibit PH growth (Liu *et al.*, 1996). Nine of these alleles are viable as haploids at 30°C, whereas three alleles (*act1-109*, *act1-110*, and *act1-131*) are recessive lethal in Σ1278b, as they are in S288c (Wertman *et al.*, 1992).

As haploids do not make florid pseudohyphae (Gimeno, *et al.*, 1992; Mösch and Fink, 1997), diploids homozygous for each of the viable alleles were constructed. Growth of all *act1/ACT1* heterozygotes and viable *act1/act1* homozygotes was assessed on YPD agar plates at 30 and 36°C to determine the recessive and dominant effects of these mutations on YF growth and viability in the Σ1278b strain background (Table 2). Strains homozygous for seven of the nine recessive viable alleles (*act1-111*, *act1-112*, *act1-113*, *act1-120*, *act1-124*, *act1-129*, and *act1-132*) exhibit temperature-sensitive growth; only two of these alleles (*act1-111*



**Table 1.** Yeast strains

Strain	Genotype	Plasmids
BCY116	MATa/MAT $\alpha$ his3::hisG/his3::hisG ura3-52/URA3 trp1::hisG/TRP1 leu2::hisG/leu2::hisG	
BCY333	MATa/MAT $\alpha$ his3::hisG/HIS3 ura3-52/ura3-52 trp1::hisG/TRP1 leu2::hisG/leu2::hisG	
BCY144	MATa/MAT $\alpha$ act1 $\Delta$ ::LEU2/ACT1 his3::hisG/his3::hisG ura3-52/URA3 trp1::hisG/TRP1 leu2::hisG/leu2::hisG	
BCY118	MATa/MAT $\alpha$ act1 $\Delta$ ::LEU2/ACT1 his3::hisG/HIS3 ura3-52/ura3-52 trp1::hisG/TRP1 leu2::hisG/leu2::hisG	pRS316
BCY156	MATa/MAT $\alpha$ act1-109::HIS3/ACT1 his3::hisG/his3::hisG ura3-52/URA3 trp1::hisG/TRP1 leu2::hisG/leu2::hisG	pIL30
BCY157	MATa/MAT $\alpha$ act1-110::HIS3/ACT1 his3::hisG/his3::hisG ura3-52/URA3 trp1::hisG/TRP1 leu2::hisG/leu2::hisG	pIL30
BCY168	MATa/MAT $\alpha$ act1-131::HIS3/ACT1 his3::hisG/his3::hisG ura3-52/URA3 trp1::hisG/TRP1 leu2::hisG/leu2::hisG	pIL30
BCY199	MATa/MAT $\alpha$ act1-124::HIS3/act1-124::HIS3 his3::hisG/his3::hisG ura3-52/URA3 trp1::hisG/TRP1 leu2::hisG/leu2::hisG	pIL30
BCY201	MATa/MAT $\alpha$ act1-113::HIS3/act1-113::HIS3 his3::hisG/his3::hisG ura 3-52/URA3 trp1::hisG/TRP1 leu2::hisG/leu2::hisG	pIL30
BCY202	MATa/MAT $\alpha$ act1-112::HIS3/act1-112::HIS3 his3::hisG/his3::hisG ura3-52/URA3 trp1::hisG/TRP1 leu2::hisG/leu2::hisG	pIL30
BCY204	MATa/MAT $\alpha$ act1-111::HIS3/act1-111::HIS3 his3::hisG/his3::hisG ura3-52/URA3 trp1::hisG/TRP1 leu2::hisG/leu2::hisG	pIL30
BCY209	MATa/MAT $\alpha$ ACT1::HIS3/ACT1::HIS3 his3::hisG/his3::hisG ura3-52/URA3 trp1::hisG/TRP1 leu2::hisG/leu2::hisG	pIL30
BCY210	MATa/MAT $\alpha$ act1-120::HIS3/act1-120::HIS3 his3::hisG/his3::hisG ura3-52/URA3 trp1::hisG/TRP1 leu2::hisG/leu2::hisG	pIL30
BCY212	MATa/MAT $\alpha$ act1-117::HIS3/act1-117::HIS3 his3::hisG/his3::hisG ura3-52/URA3 trp1::hisG/TRP1 leu2::hisG/leu2::hisG	pIL30
BCY231	MATa/MAT $\alpha$ act1-129::HIS3/act1-129::HIS3 his3::hisG/his3::hisG ura3-52/URA3 trp1::hisG/TRP1 leu2::hisG/leu2::hisG	pIL30
BCY300	MATa/MAT $\alpha$ act1-104::HIS3/act1-104::HIS3 his3::hisG/his3::hisG ura3-52/URA3 trp1::hisG/TRP1 leu2::hisG/leu2::hisG	pIL30
BCY405	MATa/MAT $\alpha$ act1-132::HIS3/act1-132::HIS3 his3::hisG/his3::hisG ura3-52/URA3 trp1::hisG/TRP1 leu2::hisG/leu2::hisG	pIL30
BCY310	MATa/MAT $\alpha$ act1-111::HIS3/act1-111::HIS3 his3::hisG/his3::hisG ura3-52/URA3 trp1::hisG/TRP1 leu2::hisG/leu2::hisG	pIL30
BCY302	MATa/MAT $\alpha$ act1-111::HIS3/act1-112::HIS3 his3::hisG/his3::hisG ura3-52/URA3 trp1::hisG/TRP1 leu2::hisG/leu2::hisG	pIL30
BCY261	MATa/MAT $\alpha$ sac6 $\Delta$ ::LEU2/SAC6 his3::hisG/HIS3 ura3-52/ura3-52 trp1::hisG/TRP1 leu2::hisG/leu2::hisG	
BCY372	MATa/MAT $\alpha$ sac6 $\Delta$ ::LEU2/sac6 $\Delta$ ::LEU2 his3::hisG/HIS3 ura3-52/ura3-52 trp1::hisG/TRP1 leu2::hisG/leu2::hisG	pRS316
BCY411	MATa/MAT $\alpha$ act1-120::HIS3/act1-120::HIS3 his3::hisG/his3::hisG ura3-52/ura3-52 trp1::hisG/trp1::hisG leu2::hisG/leu2::hisG	pIL30, AAB289, pRS314
BCY412	MATa/MAT $\alpha$ act1-120::HIS3/act1-120::HIS3 his3::hisG/his3::hisG ura3-52/ura3-52 trp1::hisG/trp1::hisG leu2::hisG/leu2::hisG	pIL30, AAB117, pRS314
BCY432	MATa/MAT $\alpha$ act1-111::HIS3/act1-111::HIS3 his3::hisG/his3::hisG ura3-52/ura3-52 trp1::hisG/TRP1 leu2::hisG/leu2::hisG	pIL30, AAB289
BCY433	MATa/MAT $\alpha$ act1-124::HIS3/act1-124::HIS3 his3::hisG/his3::hisG ura3-52/ura3-52 leu2::hisG/leu2::hisG	pIL30, AAB289

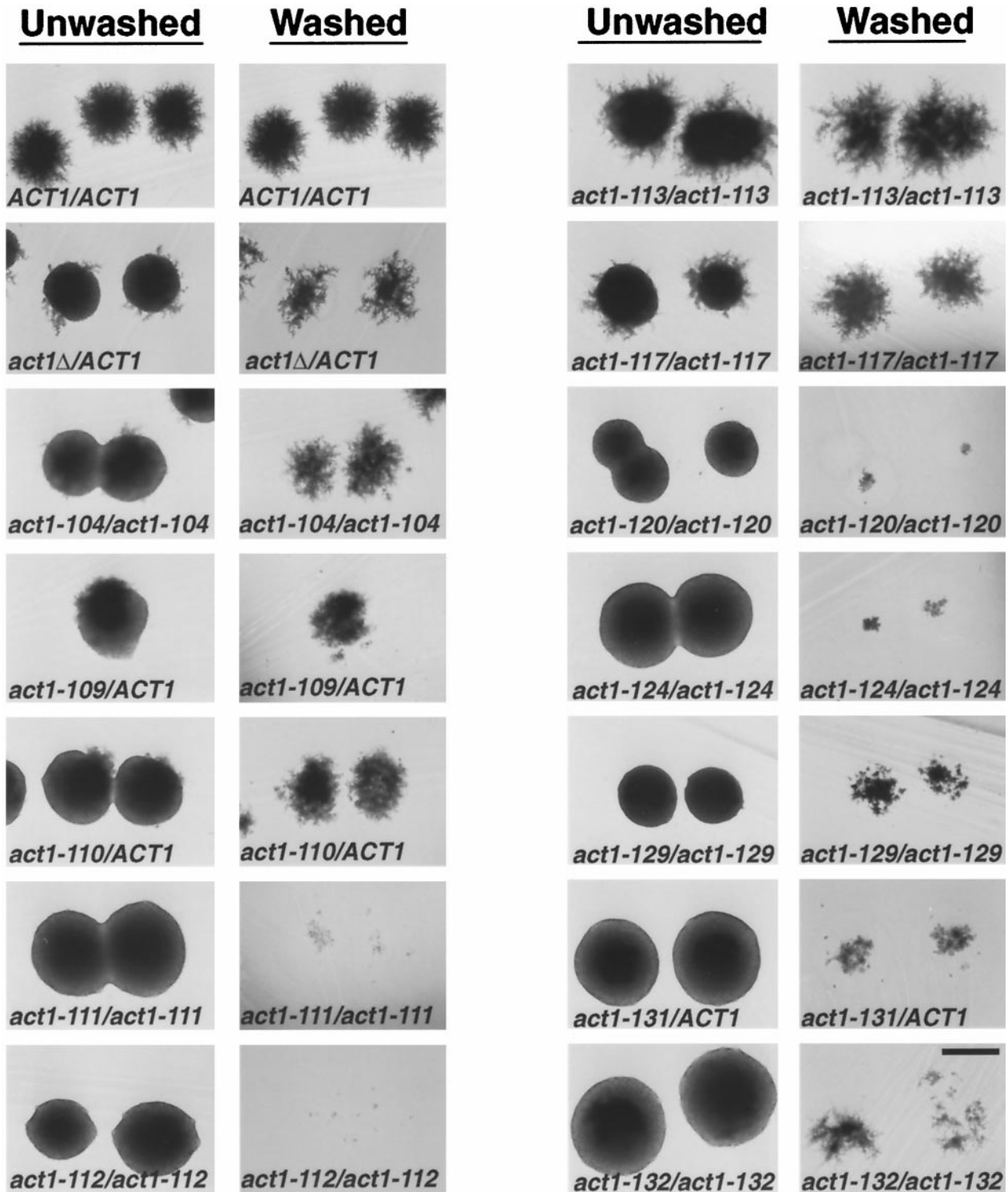
and *act1-132*) cause slow growth at 30°C. Diploids homozygous for the recessive viable alleles *act1-104* and *act1-117* grow as well as wild type at both 30 and 36°C. All alleles show the same general trends of temperature sensitivity and dominance as previously reported for these mutations in S288c with the exception of *act1-112*, which has a dominant effect on growth in  $\Sigma$ 1278b but was reported to be recessive in S288c (Wertman *et al.*, 1992).

To determine the effects of actin mutations on PH growth, strains homozygous for the recessive viable *act1* alleles and strains heterozygous for *act1 $\Delta$ ::LEU2* or the recessive lethal *act1* alleles were streaked to SLAD media to induce PH growth, and the morphology of the resulting colonies was examined after 4 d growth at 30°C (Figure 1, unwashed colonies). Of the nine viable alleles analyzed, all but *act1-113* cause filamentation defects when homozygous. The severity

of the filamentation phenotype is allele specific. For example, *act1-112/act1-112* mutants make no filaments, whereas *act1-117/act1-117* strains make many clumpy and disorganized filaments. Each of the recessive lethal alleles (*act1-109*, *act1-110*, and *act1-131*) has a dominant effect on PH growth, with *act1-131* showing the most severe phenotype. A decrease in actin dosage also has a dominant effect on PH growth, as the *act1 $\Delta$ ::LEU2/ACT1* heterozygote shows reduced filamentation. However, the phenotype of the *act1 $\Delta$ ::LEU2/ACT1* heterozygote is less severe than that of strains heterozygous for *act1-109*, *act1-110*, and *act1-131*.

#### *Allele-specific Effects of Actin Mutations on Invasion, Cell Elongation, and Unipolar Bud Site Selection*

The actin alleles were tested for their effects on other features of filamentous growth: 1) invasion—PH cells



**Figure 1.** Filamentation and invasion phenotypes of actin mutants. Strains of indicated genotype were streaked for single colonies on SLAD agar and incubated for 4 d at 30°C. Complete genotypes of strains are listed in Table 1. Colonies were photographed before (unwashed column) and after (washed column) washing the surface of the agar to remove noninvaded cells. Bar, 500  $\mu$ m.

**Table 2.** Summary of growth phenotypes of actin mutants on YPD

Allele	Growth of homozygote at 30°C	Growth of homozygote at 36°C	Dominance
WT	+++	++	
104	+++	++	
109	ND	ND	Recessive
110	ND	ND	Dominant
111	++	–	Recessive
112	+++	+/-	Dominant
113	+++	+/-	Recessive
117	+++	++	
120	+++	–	Recessive
124	+++	+/-	Recessive
129	+++	+/-	Recessive
131	ND	ND	Dominant
132	+	–	Recessive

WT, wild-type; ND, not determined, as these mutations are recessive lethal. Growth phenotypes were determined by spotting serial dilutions of a saturated culture and assessing plating efficiency and size of colonies after 3 d growth on YPD agar plates. Dominance refers specifically to effect of heterozygous mutation on growth on YPD at 36°C.

can invade the agar substrate, whereas YF cells do not; 2) cell elongation—PH cells are much longer and thinner than their YF counterparts; and 3) unipolar bud site selection—PH daughters tend to bud primarily from the pole opposite the birth end of the mother (the distal end). In contrast, YF diploids bud in a bipolar manner—the first and second daughters tend to bud from the distal end of the mother cell, and subsequent daughters bud with equal likelihood from either the proximal or distal poles. The subsequent section describes the analysis, the results of which are summarized in Table 3.

**Agar Invasion.** Colonies grown on SLAD plates were compared before and after washing (Figure 1). Five alleles (*act1-104*, *act1-109*, *act1-110*, *act1-113*, and *act1-117*) have little or no effect on agar invasion. However, the remaining seven alleles show defects ranging from a slight reduction to virtually complete elimination of agar invasion. For example, *act1-129/act1-129* homozygotes invade slightly less well than *ACT1* strains, whereas *act1-112/act1-112* homozygotes show an extreme invasion defect.

**Cell Elongation.** The percentage of long cells made under conditions that induce PH growth was determined for both the wild type and mutant strains harboring actin alanine scan alleles shown in Figure 1. The different alleles have distinct effects on elongation. Most mutants make from 30 to 80% of wild-type numbers of long cells, but *act1-112/act1-112* and *act1-120/act1-120* strains make virtually no long cells (Figure 2A).

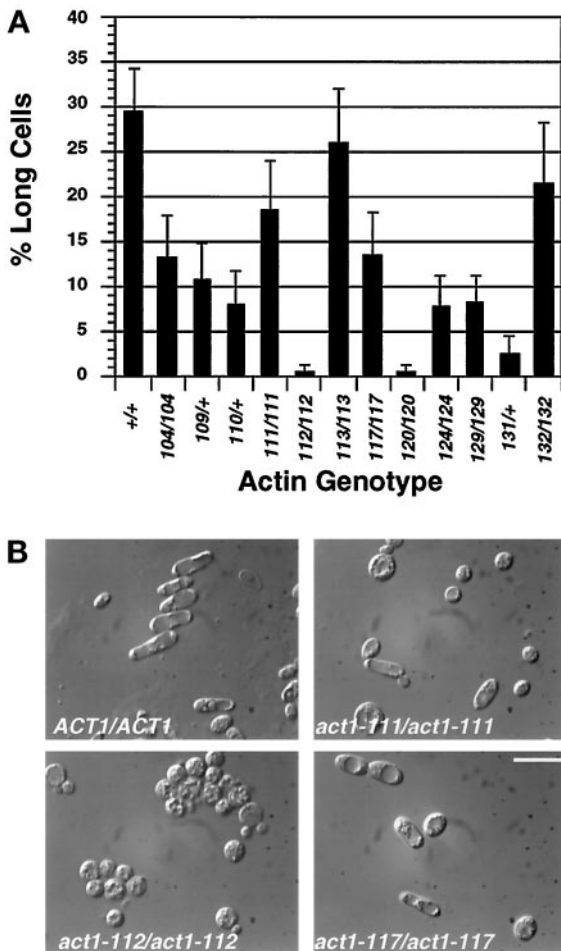
Interestingly, the effect of a given mutation on cell elongation does not correlate with its effect on invasion. For example, both *act1-111* and *act1-112* block invasion (Figure 1), but *act1-111/act1-111* strains make substantial numbers of long cells, whereas *act1-112/act1-112* homozygotes do not (Figure 2, A and B). Thus, cell elongation and invasion appear to require different functions of actin that are differentially affected by certain mutations.

**Unipolar Budding** Many mutations affecting actin (as well as mutations affecting other cytoskeletal proteins) cause random budding in YF diploids but have no effect on axial budding in haploids (Drubin *et al.*, 1993; Sivadon *et al.*, 1995; Haarer *et al.*, 1996; Zahner *et al.*, 1996; Yang *et al.*, 1997). We examined whether this subset of actin mutations affects the unipolar budding pattern that diploids exhibit during PH growth. The

**Table 3.** Summary of effects of actin mutations on filamentous growth-specific properties.

Relevant Genotype	Filamentation	Invasion	Cell Elongation	Budding Pattern
<i>ACT1/ACT1</i>	+++	+++	+++	Unipolar
<i>act1-104/act1-104</i>	+	+++	++	Unipolar
<i>act1-109/ACT1</i>	+	+++	++	Random
<i>act1-110/ACT1</i>	+	+++	+	Random
<i>act1-111/act1-111</i>	–	–	+++	ND
<i>act1-112/act1-112</i>	–	–	–	Random
<i>act1-113/act1-113</i>	+++	+++	+++	Unipolar
<i>act1-117/act1-117</i>	++	+++	++	Bipolar
<i>act1-120/act1-120</i>	–	–	–	Random
<i>act1-124/act1-124</i>	–	+	+	Random
<i>act1-129/act1-129</i>	–	++	+	Random
<i>act1-131/ACT1</i>	–	+	+	Random
<i>act1-132/act1-132</i>	–	+	+++	ND

Filamentation and invasion were scored as described in MATERIALS AND METHODS. Cell elongation scores were determined by comparing percent long cell values of mutant and wild type shown in Figure 2A. Mutants whose percent long cell value (plus the SE) was between 24 and 34% (the wild type value  $\pm$  1 SE) were scored as +++, those between 14 and 24% as ++, those between 4 and 14% as +, and those <4% as –.



**Figure 2.** Effect of *act1* mutations on cell elongation. (A) Percentage of long cells in each of the actin mutants. Complete genotypes of strains are as indicated in Figure 1. Long cell counts were performed as described in MATERIALS AND METHODS. Bars show the SE of two independent experiments. (B) Examples of different cell elongation phenotypes. Images shown are differential interference contrast images of cells scraped from the agar as above. Bar, 10  $\mu$ m.

budding patterns of 10 of the 12 *act1/act1* mutants grown under PH growth-inducing conditions were assessed (*act1-111/act1-111* and *act1-132/act1-132* homozygotes could not be scored because they exhibit abnormal chitin deposition and high background staining with calcofluor). Seven alleles cause random budding under conditions that induce PH growth, whereas three (*act1-104*, *act1-113*, and *act1-117*) do not (Table 3).

*act1-113* and *act1-117* are distinct because their effect on budding pattern is determined by nutritional conditions. *act1-113/act1-113* and *act1-117/act1-117* YF diploids were shown to bud in a random pattern in the S288c strain background (Yang *et al.*, 1997). The same alleles do not cause random budding in the

$\Sigma$ 1278b strain background under conditions that induce PH growth. Quantitative analysis of bud site selection patterns of *ACT1/ACT1*, *act1-113/act1-113*, and *act1-117/act1-117* strains grown under PH growth-inducing and noninducing conditions shows that this difference reflects an effect of growth condition, not strain background (Table 4). When grown in rich medium, *act1-113/act1-113* and *act1-117/act1-117* diploids in the  $\Sigma$ 1278b strain background show a random budding pattern similar to that seen for these alleles in S288c (Yang *et al.*, 1997). However, when grown under conditions that induce PH growth, *act1-117/act1-117* diploids exhibit a budding pattern that most closely resembles the bipolar budding pattern of wild-type YF cells. *act1-113/act1-113* diploids bud in a unipolar manner similar to that of wild-type PH cells under such conditions.

#### Intragenic Complementation between *act1* Alleles

Different *act1* alleles with similar PH phenotypes might disrupt filamentation by affecting either the same or different aspects of actin function. If two mutations affect different functions required for PH growth, then they might complement each other for filamentation defects. Mutations affecting the same functions would not. To distinguish these possibilities, all heteroallelic combinations of the nine viable *act1* alleles were constructed and tested for ability to complement each other for filamentation defects. The filamentation phenotypes of each of these strains were compared with those of strains homozygous and heterozygous for each allele (Table 5).


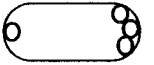

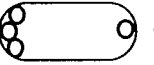
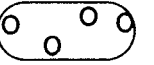
Both positive and negative interactions were observed in our complementation analysis. *act1-120*, which completely eliminates all aspects of PH growth as a homozygote, is able to complement the filamentation defects of five other *act1* alleles (*act1-104*, *act1-111*, *act1-117*, *act1-124*, and *act1-129*). An example of this effect is shown in Figure 3. Although both *act1-111/act1-111* and *act1-120/act1-120* homozygotes fail to make filaments, *act1-111/act1-120* heterozygotes exhibit filamentation indistinguishable from that of wild type. One striking negative interaction was also observed. As shown in Figure 4, *act1-111/act1-112* strains grow much more poorly at 30°C than either *act1-111/act1-111* or *act1-112/act1-112* homozygotes.

#### Dominant Effects on PH Growth

The complementation analysis also revealed that some *act1* alleles that are recessive with regard to YF growth and viability (Table 2) have dominant effects on PH growth (Table 5). Four alleles that reduce filamentation as homozygotes (*act1-112*, *act1-124*, *act1-129*, and *act1-132*) also reduce filamentation in *act1/ACT1* heterozygotes, whereas another set (*act1-104*, *act1-111*, *act1-117*, and *act1-120*) are completely recessive. We



**Table 4.** Effect of growth condition on bud-site selection in *ACT1/ACT1*, *act1-113/act1-113* and *act1-117/act1-117* diploids

Genotype	Growth Media						
<i>ACT1/ACT1</i>	YPD	3%	23%	60%	<1%	15%	(n=296)
<i>act1-113/act1-113</i>	YPD	1%	20%	22%	0%	56%	(n=337)
<i>act1-117/act1-117</i>	YPD	0%	6%	29%	<1%	65%	(n=290)
<i>ACT1/ACT1</i>	SLAD	14%	50%	33%	3%	1%	(n=303)
<i>act1-113/act1-113</i>	SLAD	10%	47%	41%	0%	2%	(n=312)
<i>act1-117/act1-117</i>	SLAD	5%	28%	52%	7%	8%	(n=200)

Exponential cultures grown in either SLAD/LA or YPD were fixed and stained with calcofluor as described in MATERIALS AND METHODS. Cells with four bud scars (or three scars and an emerging bud) were scored. The percentages of cells exhibiting the bud patterns schematized above are shown (numbers do not total to 100% because of rounding). Cells are shown with the birth end on the left.

considered the possibility that the dominance of these alleles is due to a reduction in actin dosage, as *act1Δ/ACT1* heterozygotes show a reduction in filamentation (Figure 1 and Table 5). However, strains heterozygous for *act1-112*, *act1-129*, and *act1-132* show stronger filamentation defects than the *act1Δ/ACT1* control (Table 5). This result shows that the phenotype of these heterozygotes is due to a dominant effect of the mutant actin encoded by these alleles, rather than a simple reduction in actin levels.

#### The Role of the Fimbrin–Actin Interaction in PH Growth

Although *act1-120/act1-120* homozygotes are defective for all aspects of PH growth investigated, this

allele complements the PH growth defects of many other actin mutants (Table 5). Thus, *act1-120* appears to encode a mutant actin that retains substantial function. Genetic and biochemical studies in yeast have established that *act1-120* perturbs binding of the actin filament-bundling protein fimbrin (Sac6p) both in vitro and in vivo (Holtzman *et al.*, 1994; Honts *et al.*, 1994, Sandrock *et al.*, 1997, Doyle and Botstein, unpublished observations). This is consistent with structural data showing that the residues affected by *act1-120* (E99 and E100) are in a region of subdomain 1 of actin that forms extensive contacts with the amino-terminal domain of fimbrin (Hanein *et al.*, 1997). Specific mutations affecting either of the two actin-binding domains of fimbrin can suppress the temperature-sensi-

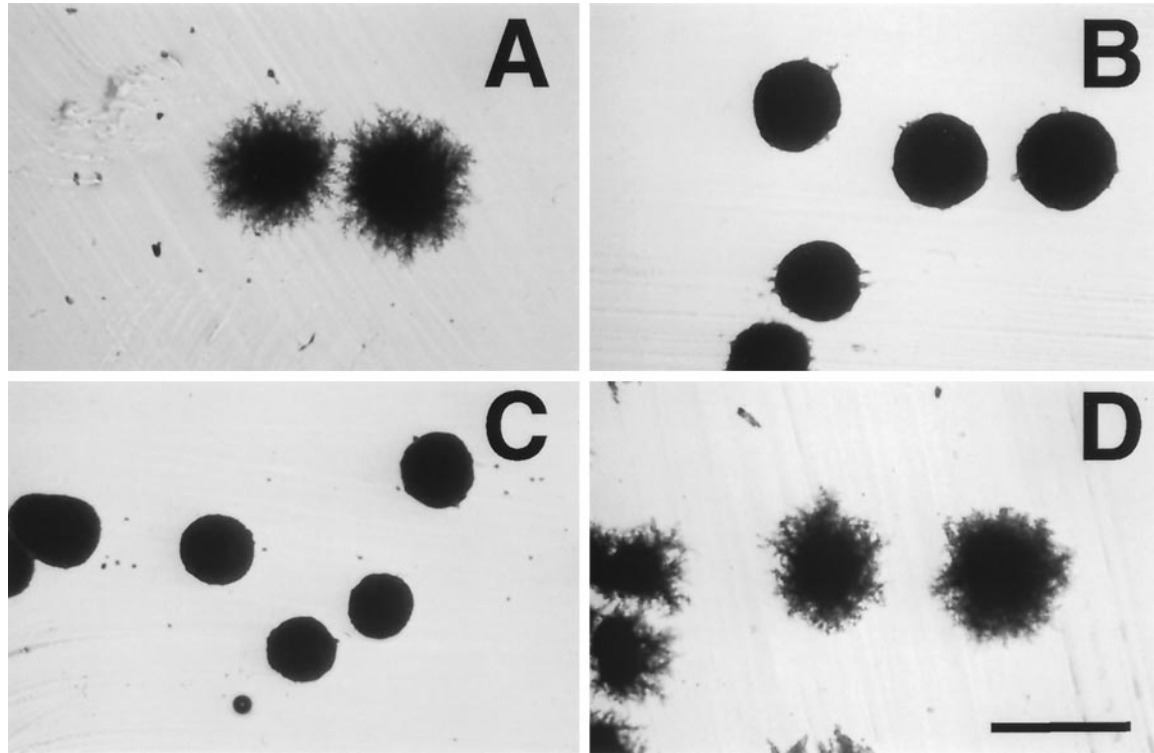
**Table 5.** Filamentation phenotypes of *act1* allelic combinations

Allele	WT	Δ	104	111	112	113	117	120	124	129	132
WT	+++	++	+++	+++	–	+++	+++	+++	++	+	+
104			+	+	–	++	+	+++	+	–	–
111				–	– <sup>a</sup>	+++	++	+++	–	–	–
112					–	–	–	–	–	–	–
113						+++	+++	+++	++	+	+
117							++	+++	+	–	+
120								–	+	+	–
124									–	–	–
129										–	–
132											–

Filamentation of heteroallelic *act1/act1* diploids was scored after 4 d growth at 30°C on SLAD agar plates as described in MATERIALS AND METHODS. WT, wild type.

<sup>a</sup> Very poor growth of heteroallelic strain at 30°C (see Figure 4).





**Figure 3.** *act1-111* and *act1-120* exhibit intragenic complementation for filamentation defects. Shown is the growth on SLAD agar after four days at 30°C. (A) BCY209 (*ACT1/ACT1*); (B) BCY204 (*act1-111/act1-111*); (C) BCY210 (*act1-120/act1-120*); (D) BCY310 (*act1-111/act1-120*). Bar, 500  $\mu\text{m}$ .

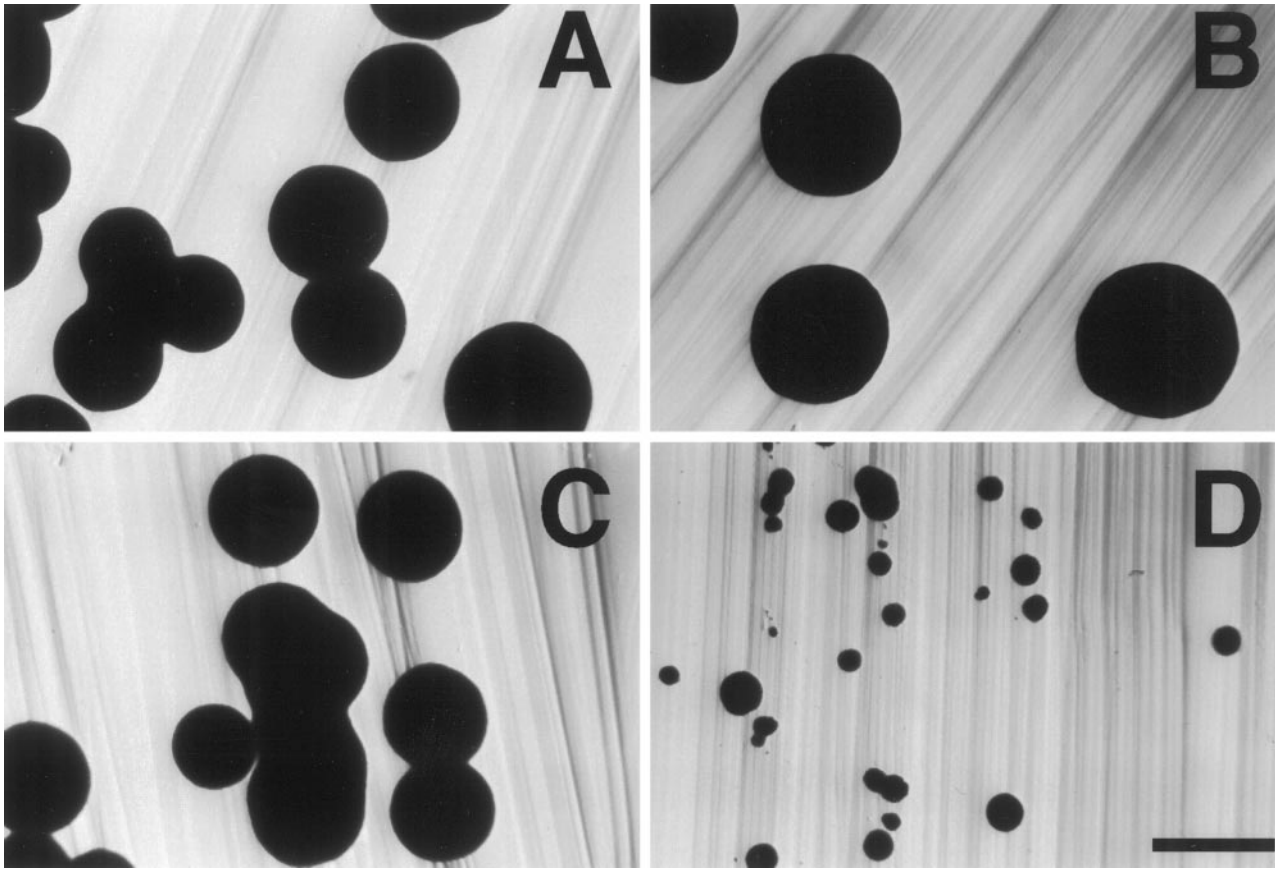
tive lethal phenotype of *act1-120* (Brower *et al.*, 1995; Sandroock *et al.*, 1997).

We propose that the major effect of *act1-120* on PH growth is through its effect on fimbrin binding. This model can be directly tested by evaluating two important predictions: 1) *sac6/sac6* and *act1-120/act1-120* mutants will show similar PH growth defects; and 2) *sac6* alleles that restore the interaction between fimbrin and the mutant actin encoded by *act1-120* will suppress some or all of the PH growth defects of *act1-120/act1-120* mutants. Both of these predictions are borne out. As shown in Figure 5, *sac6* $\Delta$ ::*LEU2/sac6* $\Delta$ ::*LEU2* diploids, like *act1-120/act1-120* mutants, make no filaments, are invasion defective, and are severely reduced for cell elongation at 30°C. Expression of a mutant fimbrin encoded by *sac6-10* rescues both the cell elongation and invasion phenotypes of these mutants. *sac6-10* alters a conserved tryptophan in the first actin binding domain of fimbrin (W252C) and was shown to suppress the temperature-sensitive phenotype of *act1-120*, presumably by restoring the fimbrin-actin interaction (Brower *et al.*, 1995; Sandroock *et al.*, 1997). Importantly, *sac6-10* does not suppress the PH growth defects of two actin mutations (*act1-111* and *act1-124*) that affect residues in subdomains 4 and 2, respectively, and are not predicted to interfere with fimbrin binding

to actin. These data indicate that the invasion and cell elongation phenotypes of *act1-120/act1-120* mutants are due primarily to a defect in fimbrin binding.

#### *Characterization of the Actin Cytoskeleton in PH Cells in Wild Type and act1 Mutants*

As a basis for understanding the similarities and differences in the YF and PH actin cytoskeletons and how this may account for the differences in cell shape and other growth properties in these distinct cell types, the actin cytoskeleton was imaged in both YF and PH cells at various stages of the cell cycle (Figure 6). The major structural features of the PH and YF actin cytoskeletons are similar in that a prominent ring of filamentous actin is seen at the site of bud emergence, cortical patches are found almost exclusively in the emerging bud, and cables are oriented toward the site of bud emergence in both mother and daughter cells. However, there are notable differences in cytoskeletal structure between these cell types that bear mention. As observed previously (Kron *et al.*, 1994), we find that the polarity of patch localization is enhanced in PH cells relative to YF cells, as patches tend to remain at the distal pole throughout bud emergence in PH cells until a new ring of filamentous actin is formed at the



**Figure 4.** *act1-111* and *act1-112* exhibit a negative growth interaction. Shown are colonies after growth for 3 d at 30°C on YNB. (A) BCY209 (*ACT1/ACT1*); (B) BCY204 (*act1-111/act1-111*); (C) BCY202 (*act1-112/act1-112*); (D) BCY302 (*act1-111/act1-112*). Bar, 1 mm.


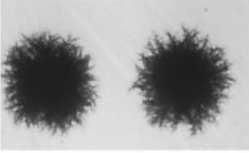
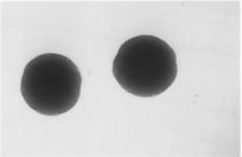
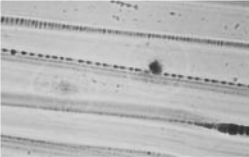
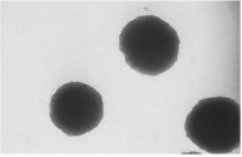

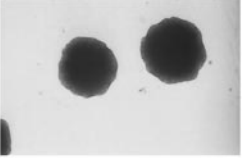
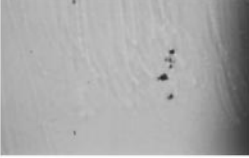
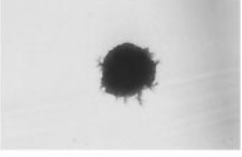

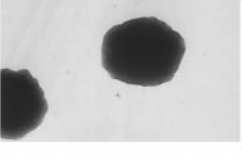

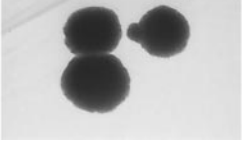
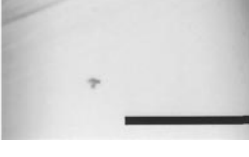
eventual site of cytokinesis. In addition, actin cables are more pronounced in PH cells than in YF cells.

As was recently shown for YF cells in the S288c background (Botstein *et al.*, 1997), we find that actin cables are cortical in both YF and PH cells in the  $\Sigma$ 1278b genetic background. Cables appear to run just under the plane in which patches reside and to follow the overall contour of the cell. Thus, it appears generally true that actin cables do not run directly through the cytoplasm as has long been thought. It seems likely that the cortical nature of actin cables was not noticed previously because the generation and manipulation of high resolution stereo images of the yeast actin cytoskeleton has only recently become possible.

Actin patch dynamics were also examined in wild-type PH cells using a previously described GFP-SAC6 fusion (Doyle and Botstein, 1996). Expression of this fusion protein rescues all PH growth defects associated with deletion of *SAC6*, providing additional evidence to that previously presented that this fusion protein is fully functional (Doyle and Botstein, 1996). Analysis of actin patch dynamics showed that actin patches are mobile in PH cells, as they are in YF cells

(Doyle and Botstein, 1996; Waddle *et al.*, 1996). Patch dynamics did not appear to differ significantly between YF and PH cells.

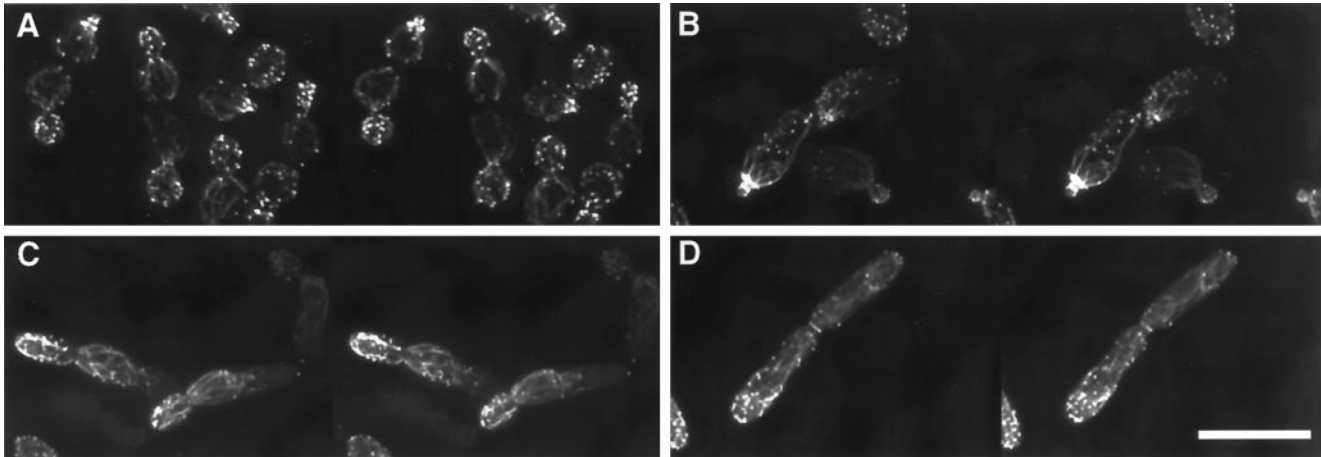
Rhodamine-phalloidin staining of all *act1/act1* mutants (with the exception of *act1-129*, which encodes an actin that does not bind phalloidin; Drubin *et al.*, 1993) grown under PH growth-inducing conditions revealed numerous defects in actin cytoskeletal structure. Cytoskeletal structure in a sample of mutants is shown in Figure 7. (Rotations of these mutants and of the wild-type PH cells in Figure 6 further illustrate many of the features of the actin cytoskeleton discussed here and are available on the internet version of this manuscript.) In all mutants with effects on PH growth, actin cables are either absent or thin and disorganized. Perturbation of actin patch polarization and morphology was also observed, with the most pronounced effects in those mutants displaying the most severe cell elongation defects. For example, in *act1-120/act1-120* homozygotes and *act1-131/ACT1* heterozygotes, which both show strong defects in cell elongation (Figure 2), actin patches are depolarized and located in both mother and daughter cells. *act1-*

	<u>Unwashed</u>	<u>Washed</u>	<u>% Long Cells</u>
<i>ACT1</i> <i>ACT1</i>			<b>53.0 ± 6.7</b>
<i>act1-120</i> <i>act1-120</i>			<b>2.0 ± 2.7</b>
<i>sac6Δ::LEU2</i> <i>sac6Δ::LEU2</i>			<b>4.2 ± 2.9</b>
<i>act1-120</i> <i>act1-120</i> < <i>SAC6+</i> >			<b>1.5 ± 1.7</b>
<i>act1-120</i> <i>act1-120</i> < <i>sac6-10</i> >			<b>32.0 ± 6.4</b>
<i>act1-111</i> <i>act1-111</i> < <i>sac6-10</i> >			<b>19.0 ± 3.4</b>
<i>act1-124</i> <i>act1-124</i> < <i>sac6-10</i> >			<b>6.2 ± 2.5</b>

**Figure 5.** Expression of a mutant fimbrin (Sac6p) with an altered actin-binding domain suppresses the invasion and cell elongation defects of an *act1-120/act1-120* diploid. Strains BCY209 (*ACT1/ACT1*), BCY210 (*act1-120/act1-120*), BCY372 (*sac6/sac6*), BCY412 (*act1-120/act1-120* <*SAC6+*>), BCY411 (*act1-120/act1-120* <*sac6-10*>), BCY432 (*act1-111/act1-111* <*sac6-10*>), and BCY433 (*act1-124/act1-124* <*sac6-10*>), where genotypes in angle brackets refer to relevant genotypes of plasmids AAB117 (*SAC6 URA3 CEN*) and AAB289 (*sac6-10 URA3 CEN*) (Brower *et al.*, 1995), were streaked to SLAD agar and incubated at 30°C for 4 d. The resultant colonies were photographed before and after washing the agar surface. Long cells were quantified as described in MATERIALS AND METHODS and are reported with SE. Bar, 500 μm.

*112/act1-112* homozygotes, which are also severely affected in cell elongation, show defects in patch polarization, an overall reduction in patch number and staining intensity, and a large proportion of cells with thick or clumpy patches (Figure 7). Multibudded and

multinucleate cells were also apparent in many mutants under PH growth-inducing conditions (e.g., *-act1-120/act1-120* and *act1-112/act1-112* in Figure 7). The abnormal patch structures and nuclear segregation and budding defects we observed under these



**Figure 6.** Comparison of the YF and PH actin cytoskeletons. Stereo images of the filamentous actin cytoskeleton (stained with rhodamine-phalloidin) in strain BCY209 grown either in YPD (A) or in SLAD alginate (B–D). (A) YF cells: all stages of cell cycle. (B) PH cell, early bud emergence; note prominent ring of actin in mother cell at site of bud emergence and at the neck of the very small emerging bud. (C) PH cell, midbud emergence; image shows the pronounced actin cables and patch polarization to the distal end of the emerging bud. (D) PH cell shortly before cytokinesis; a ring of actin has formed at the septation site between mother and daughter, whereas some patches remain near the distal end of the daughter cell. Bar, 10  $\mu$ m.

conditions closely resemble those previously described for these and other *act1* mutants in YF cells (Drubin *et al.*, 1993).

For those mutants capable of making long cells, actin patch polarization is more normal under PH growth-inducing conditions than for those mutants with the most severe cell elongation defects. For example, *act1-111/act1-111* homozygotes and *act1-110/ACT1* heterozygotes both show relatively normal patch morphology and polarization in long cells (Figure 7), whereas actin cables are rarely seen in these mutants. These data underscore the importance of patch polarization to the distal end of the emerging bud for cell elongation during PH growth (see DISCUSSION).

## DISCUSSION

### *Actin Has Multiple Functions in Filamentous Growth*

We have shown that *act1* mutations disrupt the PH growth-specific properties of agar invasion, cell elongation, and unipolar bud site selection. Some *act1* mutations show allele-specific effects on invasion, cell elongation, and unipolar budding (Table 3). In addition, certain *act1* mutations exhibit specific intragenic complementation with respect to PH growth defects (Table 5). These data suggest that there are multiple requirements for actin function in PH growth.

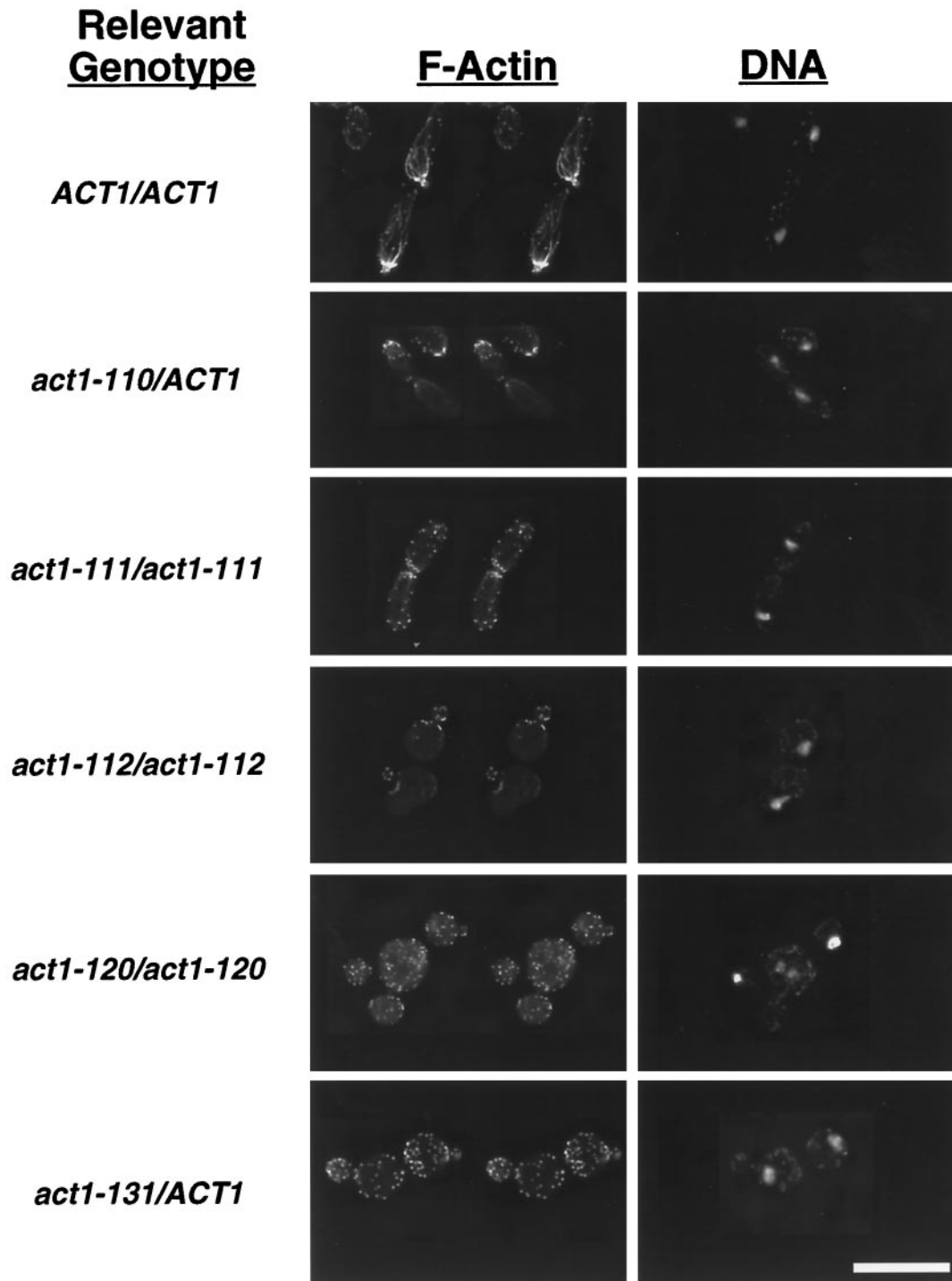
Several observations indicate that the effects of these mutations on PH growth are due to specific effects on functions of actin required for PH growth and not general effects on cell growth and physiology. First,

two alleles that have no effect on viability at any temperature (*act1-104* and *act1-117*) both exhibit pronounced effects on filamentation. Second, filamentation defects are seen at the “permissive” temperature (30°C) for the temperature-sensitive *act1* alleles and the *sac6* mutant analyzed in this study. Third, only two alleles analyzed in this study (*act1-111* and *act1-132*) show obvious growth defects at the temperature at which these studies were conducted (30°C) (Table 2), and these mutations have less severe effects on PH growth than other alleles with no overt growth phenotypes at this temperature (e.g., *-act1-112* and *act1-120*) (Table 3).

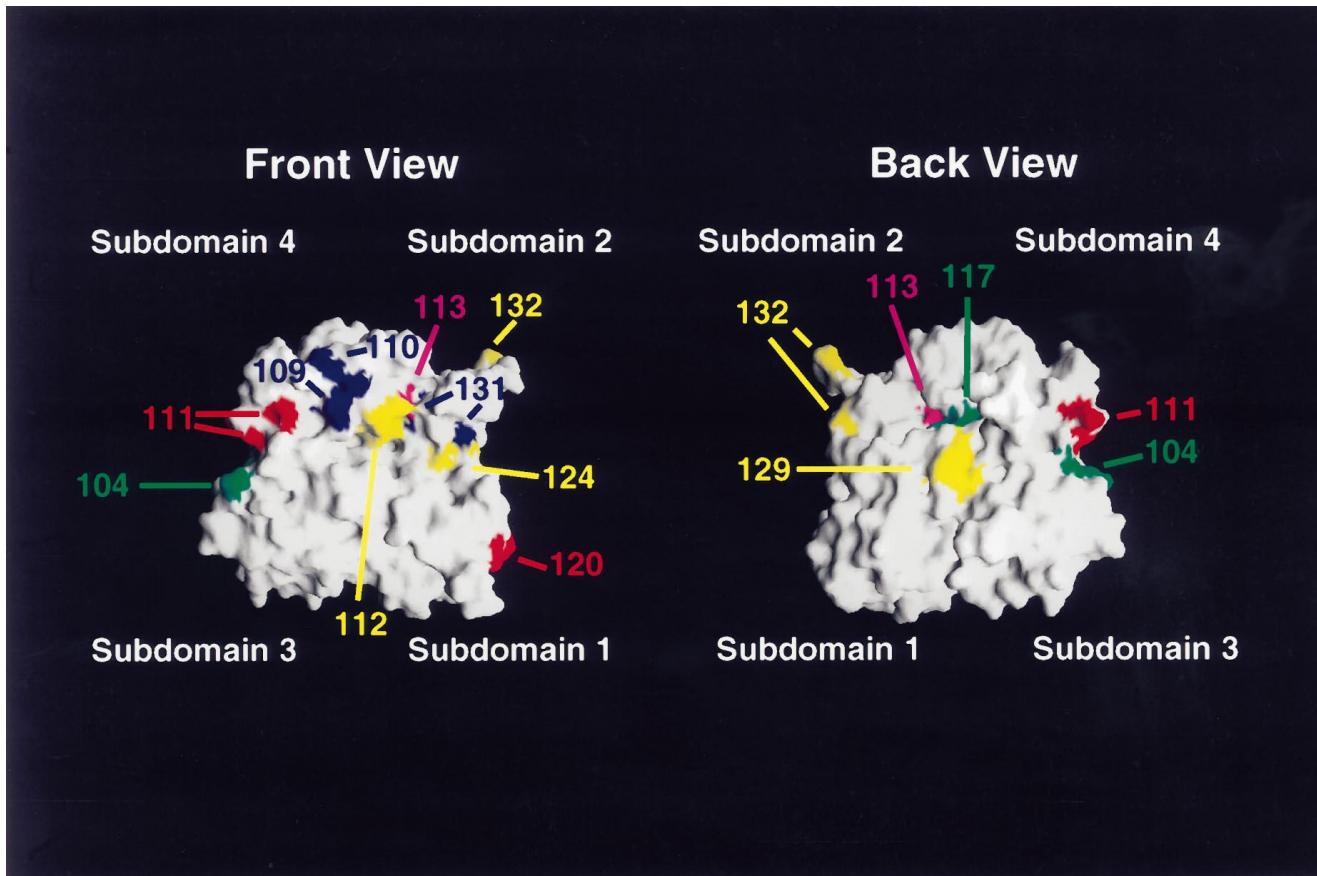
### *The Utility of Filamentous Growth for Studying Actin Function*

Filamentous growth provides a uniquely sensitive assay for actin cytoskeletal function during a developmental switch. The sensitivity of this system allowed us to identify new phenotypic consequences for mutations affecting actin. We found dominant effects on filamentation for several actin mutations previously classified as recessive based on their effects on YF growth. Effects on PH growth were also found for certain *act1* alleles that have no (or subtle) effects on YF growth and viability. In addition, using the filamentation phenotype, we have been able to identify genetic interactions between actin alleles. Similar efforts to define *act1* intragenic complementation by assessing growth at restrictive temperature have led to ambiguous results.





**Figure 7.** The actin cytoskeleton in actin mutants grown under conditions that induce PH growth. Shown are wild-type and actin mutant strains grown in SLAD alginate and stained with rhodamine-phalloidin (to detect F-actin) and DAPI (to detect DNA) as described in MATERIALS AND METHODS. F-actin images are in stereo. Strains shown are BCY209 (*ACT1/ACT1*), BCY157 (*act1-110/ACT1*), BCY204 (*act1-111/act1-111*), BCY202 (*act1-112/act1-112*), BCY210 (*act1-120/act1-120*), and BCY168 (*act1-131/ACT1*). Bar, 10  $\mu$ m.



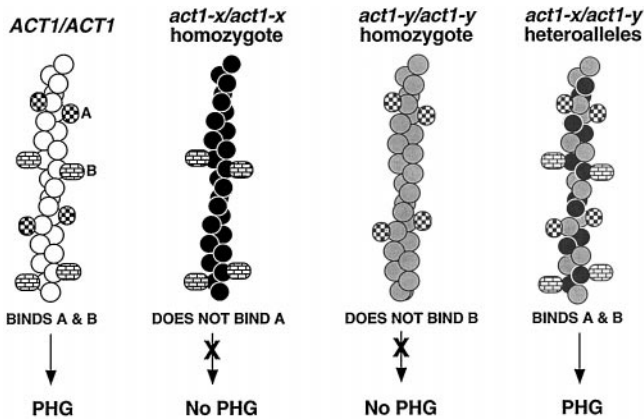
**Figure 8.** Modeling of the mutations analyzed in this study onto the solvent-exposed surface of an actin monomer. Shown is the calculated surface of the actin monomer based on the coordinates of the rabbit muscle actin filament structure (Lorenz *et al.*, 1993). Actin subdomains are indicated. Red, locations of residues altered by viable, temperature-sensitive alleles with recessive effects on PH growth; yellow, location of residues altered by viable, temperature-sensitive alleles with dominant effects on PH growth; blue, positions of residues affected by recessive lethal alleles with dominant effects on PH growth; green, locations of residues affected by mutations that have no effect on viability but disrupt PH growth; magenta, positions of residues altered by mutations with no effect on PH growth. Surfaces were generated using GRASP (Nicholls *et al.*, 1991) on a Silicon Graphics Iris computer.

### *New Insights into Actin Structure and Function Revealed by Analysis of PH Growth Phenotypes*

Many actin mutations are likely to cause defects in PH growth by blocking the interaction between actin and other proteins. Indeed, we have shown that *act1-120*, which is known to disrupt binding of fimbrin to actin, can be suppressed for its invasion and cell elongation defects by a compensatory mutation in the actin-binding domain of fimbrin (Figure 5). Other *act1* alleles with effects on PH growth are known or presumed to affect the binding of proteins required for filamentation, suggesting that the phenotypes of these *act1* mutants may be also be due, in part, to an effect on the binding of these proteins. For example, *act1-110* alters residues (E237 and K238) that are part of the binding site for the actin filament-stabilizing protein tropomyosin (Milligan *et al.*, 1990; Saeki *et al.*, 1996), which is encoded by *TPM1* and *TPM2* in yeast (Drees *et al.*,

1995). *tpm1/tpm1* mutants, like *act1-110/ACT1* heterozygotes, are defective for filamentation (Mösch and Fink, 1997). *act1-104* is particularly interesting, in that this allele has no known YF phenotype and is not known to affect the binding of any actin-binding protein, yet it has an obvious effect on filamentation. *act1-104* alters residues (K315 and E316) predicted to lie on the surface of both the actin monomer (Figure 8) and the actin filament. Thus, these amino acids are well positioned to be a binding site for an as yet unidentified protein with a specific role in PH growth.

Several mutations may act by altering the interaction of actin with itself. Four alleles that show effects on PH growth (*act1-111*, *act1-112*, *act1-129*, and *act1-132*) disrupt actin-actin interactions in the two-hybrid assay (Amberg *et al.*, 1995) and alter residues predicted to stabilize actin-actin contacts (Holmes *et al.* 1990; Lorenz *et al.*, 1993). Actin monomers defective



**Figure 9.** Model for mechanism of intragenic complementation between *act1* alleles (after Ayscough and Drubin, 1996). Actin monomers encoded by *ACT1*, *act1-x*, and *act1-y* are represented by white, black, and gray circles, respectively. The ability of hypothetical actin-binding proteins A and B to interact with actin filaments comprising wild-type actin, each mutant actin singly, or a combination of mutant actins is schematized. The PH growth phenotype of strains containing such actin filaments is also indicated.

for one such interaction could disrupt filament assembly in a dominant manner by their incorporation into a growing filament and blocking additional contacts necessary for filament stability and/or elongation. Interestingly, three alleles that affect actin-actin contacts (*act1-112*, *act1-129*, and *act1-132*) do indeed show dominant effects on PH growth.

The synthetic growth defect of *act1-111/act1-112* (Figure 4) may also be explained by effects on actin filament assembly and stability. Insertion of a hydrophobic loop from one actin monomer into a hydrophobic hole defined in part by the cleft between subdomains 2 and 4 in an adjacent actin monomer has been suggested to stabilize interactions within the actin filament (Chen *et al.*, 1993; Lorenz *et al.*, 1993; Kuang and Rubenstein, 1997). *act1-111* affects amino acids (D222, E224, and E226) that form a pocket in which the hydrophobic loop resides in monomeric actin and may perturb the ability of the hydrophobic loop to swing out of the pocket to interact with the hydrophobic cleft (Amberg *et al.*, 1995). *act1-112* alters residues (K213, E214, and K215) that form one-half of the cleft into which the hydrophobic loop is inserted. Thus, the negative interaction between these alleles could reflect a synergistic effect of perturbing both structural features required for filament stability.

The demonstration that some *act1* mutations exert their effects by altering the binding of specific actin-binding proteins suggests a mechanism for the intragenic complementation we have observed. Such alleles might allow formation of heteropolymeric actin filaments that can bind ligands that neither homopolymer can bind. For example, as shown in Figure 9, two

actin alleles (X and Y) might affect binding of distinct proteins (A and B) that are both required for filamentation. If allele X blocks binding of A, and allele Y blocks binding of B, *act1-x/act1-x* and *act1-y/act1-y* homozygotes would be defective for PH growth, but because of distinct molecular effects. However, actin filaments comprising X and Y monomers would be competent to bind both A and B, and so *act1-x/act1-y* strains would exhibit filamentation. Intragenic complementation between *act1* alleles based on such a mechanism has been predicted (Ayscough and Drubin, 1996). However, to our knowledge the data presented here represent the first experimental demonstration of this effect.

This model predicts that mutations exhibiting intragenic complementation should affect binding of distinct subsets of ligands and will likely reside in different regions of the actin monomer and/or filament. Indeed, *act1-120* is the only mutant analyzed in this study localized to subdomain 1 of actin (Figure 8), and it is able to complement mutations in subdomains 2, 3, and 4 that are quite distant (in both the monomer and filament) from those mutations it complements for PH growth defects (*act1-104* [subdomain 3], *act1-111* [subdomain 4], *act1-117* [subdomain 4], *act1-124* [subdomain 2], and *act1-129* [subdomain 3]). In addition, in the two-hybrid assay, the actin encoded by *act1-120* binds many ligands whose binding was disrupted by *act1* mutations that *act1-120* can complement (Amberg *et al.*, 1995).

#### *Actin Function in Cell Elongation, Unipolar Budding, and Agar Invasion*

Our results suggest that cytoskeletal integrity is essential for filamentation. What might be the specific requirements for actin in each of the PH growth-specific traits we analyzed?

**Cell Elongation.** The PH and YF actin cytoskeletons are different in structure. In YF cells, there is a distinct period during bud emergence in which actin patches are distributed over the cortex of the emerging bud. In PH cells, actin patches remain polarized at the tip of the cell throughout bud emergence (Kron *et al.*, 1994). Our imaging of the PH actin cytoskeleton in wild type and *act1* mutants confirms and extends this observation to suggest that actin patch polarization plays an important role in the elongation of the PH cell. In *act1/act1* mutants with the most pronounced effects on cell elongation (*act1-112/act1-112* and *act1-120/act1-120* homozygotes and *act1-131/ACT1* heterozygotes), substantial perturbation of actin patch polarization during bud emergence is observed (Figure 7). In contrast, actin patches are polarized to the distal end of many emerging buds in those actin mutants capable of making substantial numbers of long cells. These results are consistent with the proposal that actin

patches play an important role in directing secretion of new membrane and cell wall material in the emerging bud (Novick and Botstein, 1985; Mulholland *et al.*, 1994). Thus, the extended polarization of actin patches to the distal end of PH cells throughout bud emergence would promote elongation of the PH cell.

**Unipolar Budding.** The demonstration that actin cytoskeletal mutants are unable to exhibit bipolar budding in YF cells led to the suggestion that the actin cytoskeleton is required to maintain, and perhaps direct, the placement of bipolar bud site selection cues (Zahner *et al.*, 1996; Yang *et al.*, 1997). These presently unidentified signals, present at both the proximal and distal ends of the cell, would then serve to direct new bud formation at either end of the mother cell. The fact that nearly all actin mutants we characterized exhibit random budding under conditions that induce PH growth demonstrates that, like bipolar bud site selection in YF diploids, unipolar bud site selection in PH cells requires actin cytoskeletal function. However, *act1-113/act1-113* and *act1-117/act1-117* strains are suppressed for their YF random budding phenotype when grown under conditions that induce PH growth (Table 4). Thus, despite their similar dependency for actin function, these results demonstrate that the YF and PH bud site selection programs are regulated somewhat distinctly in response to nutrient conditions.

**Invasion.** The mechanism by which PH cells invade agar is not known. However, it has been suggested that these cells might secrete enzymes that hydrolyze agar and thus facilitate growth through the substrate (Gimeno *et al.*, 1992). Indeed, many invasive fungi, including *Candida albicans*, have been shown to secrete proteases and other enzymes believed to facilitate their invasion (Macdonald and Odds, 1983). Given the well-established role for actin in secretion, it is tempting to speculate that actin is required for the secretion of such enzymes.

## ACKNOWLEDGMENTS

We thank Alison Adams for plasmids used in this work, Ken Holmes for the actin filament coordinates, and James Berger for assistance using GRASP. We are grateful to members of the Fink and Botstein laboratories for helpful discussions and Todd Milne for critical reading of the manuscript. Many thanks to Katja Schwartz for providing help with some of the microscopy in Figure 6. B.M.C. is a Chiron Fellow of the Life Sciences Research Foundation. G.R.F. is an American Cancer Society Professor of Genetics. The DeltaVision microscope system is supported by National Institutes of Health Research Resources grant RR11939-01. This work was supported by grants from the National Institutes of Health (GM46406-07 to D.B. and GM35010 to G.R.F.).

## REFERENCES

Adams, A.E., and Botstein, D. (1989). Dominant suppressors of yeast actin mutations that are reciprocally suppressed. *Genetics* 121, 675–683.

Adams, A.E., Botstein, D., and Drubin, D.G. (1989). A yeast actin-binding protein is encoded by *SAC6*, a gene found by suppression of an actin mutation. *Science* 243, 231–233.

Adams, A.E. and Pringle, J.R. (1984). Relationship of actin and tubulin distribution to bud growth in wild-type and morphogenetic-mutant *Saccharomyces cerevisiae*. *J. Cell Biol.* 98, 934–945.

Adams, A.E., Shen, W., Lin, C.S., Leavitt, J., and Matsudaira, P. (1995). Isoform-specific complementation of the yeast *sac6* null mutation by human fimbrin. *Mol. Cell Biol.* 15, 69–75.

Agard, D.A., Hiraoka, Y., Shaw, P., and Sedat, J.W. (1989). Fluorescence microscopy in three dimensions. *Methods Cell Biol.* 30, 353–377.

Amatruda, J.F., Cannon, J.F., Tatchell, K., Hug, C., and Cooper, J.A. (1990). Disruption of the actin cytoskeleton in yeast capping protein mutants. *Nature* 344, 352–354.

Amberg, D.C., Basart, E., and Botstein, D. (1995). Defining protein interactions with yeast actin in vivo. *Nat. Struct. Biol.* 2, 28–35.

Amberg, D.C., Zahner, J.E., Mulholland, J.W., Pringle, J.R., and Botstein, D. (1997). Aip3p/Bud6p, a yeast actin-interacting protein that is involved in morphogenesis and the selection of bipolar budding sites. *Mol. Biol. Cell* 8, 729–753.

Ayscough, K.R., and Drubin, D.G. (1996). ACTIN: general principles from studies in yeast. *Annu. Rev. Cell. Dev. Biol.* 12, 129–160.

Botstein, D., Amberg, D., Mulholland, J., Huffaker, T., Adams, A., Drubin, D., and Stearns, T. (1997). The yeast cytoskeleton. In: *The molecular and cellular biology of the yeast Saccharomyces: cell cycle and cell biology*, vol 3, ed. J.R. Pringle, J.R. Broach, and E.W. Jones, Cold Spring Harbor, NY: Cold Spring Harbor Press, 1–90.

Brower, S.M., Honts, J.E., and Adams, A.E. (1995). Genetic analysis of the fimbrin-actin binding interaction in *Saccharomyces cerevisiae*. *Genetics* 140, 91–101.

Chen, X., Cook, R.K., and Rubenstein, P.A. (1993). Yeast actin with a mutation in the “hydrophobic plug” between subdomains 3 and 4 (L266D) displays a cold-sensitive polymerization defect. *J. Cell Biol.* 123, 1185–1195.

Doyle, T., and Botstein, D. (1996). Movement of yeast cortical actin cytoskeleton visualized in vivo. *Proc. Natl. Acad. Sci. USA* 93, 3886–3891.

Drees, B., Brown, C., Barrell, B.G., and Bretscher, A. (1995). Tropomyosin is essential in yeast, yet the *TPM1* and *TPM2* products perform distinct functions. *J. Cell Biol.* 128, 383–392.

Drubin, D.G., Jones, H.D., and Wertman, K.F. (1993). Actin structure and function: roles in mitochondrial organization and morphogenesis in budding yeast and identification of the phalloidin-binding site. *Mol. Biol. Cell* 4, 1277–1294.

Drubin, D.G., Miller, K.G., and Botstein, D. (1988). Yeast actin-binding proteins: evidence for a role in morphogenesis. *J. Cell Biol.* 107, 2551–2561.

Drubin, D.G., Mulholland, J., Zhu, Z.M., and Botstein, D. (1990). Homology of a yeast actin-binding protein to signal transduction proteins and myosin-I. *Nature* 343, 288–290.

Gietz, D., St. Jean, A., Woods, R.A., and Schiestl, R.H. (1992). Improved method for high efficiency transformation of intact yeast cells. *Nucleic Acids Res.* 20, 1425.

Gimeno, C.J., Ljungdahl, P.O., Styles, C.A., and Fink, G.R. (1992). Unipolar cell divisions in the yeast *S. cerevisiae* lead to filamentous growth: regulation by starvation and RAS. *Cell* 68, 1077–1090.

Guthrie, C., and Fink, G.R. (1991). *Guide to yeast genetics and molecular biology*. San Diego: Academic Press.

Haarer, B.K., Corbett, A., Kweon, Y., Petzold, A.S., Silver, P., and Brown, S.S. (1996). *SEC3* mutations are synthetically lethal with



- profilin mutations and cause defects in diploid-specific bud-site selection. *Genetics* 144, 495–510.
- Hanein, D., Matsudaira, P., and DeRosier, D.J. (1997). Evidence for a conformational change in actin induced by fimbrin (N375) binding. *J. Cell Biol.* 139, 387–396.
- Holmes, K.C., Popp, D., Gebhard, W., and Kabsch, W. (1990). Atomic model of the actin filament. *Nature* 347, 44–49.
- Holtzman, D.A., Wertman, K.F., and Drubin, D.G. (1994). Mapping actin surfaces required for functional interactions in vivo. *J. Cell Biol.* 126, 423–432.
- Honts, J.E., Sandrock, T.S., Brower, S.M., O'Dell, J.L., and Adams, A.E. (1994). Actin mutations that show suppression with fimbrin mutations identify a likely fimbrin-binding site on actin. *J. Cell Biol.* 126, 413–422.
- Ito, H., Fukuda, Y., Murata, K., and Kimura, A. (1983). Transformation of intact yeast cells treated with alkali cations. *J. Bacteriol.* 153, 163–168.
- Kron, S.J., Styles, C.A., and Fink, G.R. (1994). Symmetric cell division in pseudohyphae of the yeast *Saccharomyces cerevisiae*. *Mol. Biol. Cell* 5, 1003–1022.
- Kuang, B., and Rubenstein, P.A. (1997). Beryllium fluoride and phalloidin restore polymerizability of a mutant yeast actin (V266G, L267G) with severely decreased hydrophobicity in a subdomain 3/4 loop. *J. Biol. Chem.* 272, 1237–1247.
- Laloux, I., Jacobs, E., and Dubois, E. (1994). Involvement of SRE element of Ty1 transposon in TEC1-dependent transcriptional activation. *Nucleic Acids Res.* 22, 999–1005.
- Law, D.J., and Reed, S.I. (1993). Morphogenesis in the yeast cell cycle: regulation by Cdc28 and cyclins. *J. Cell Biol.* 120, 1305–1320.
- Liu, H., Styles, C.A., and Fink, G.R. (1996). *Saccharomyces cerevisiae* S288C has a mutation in *FLO8*, a gene required for filamentous growth. *Genetics* 144, 967–978.
- Liu, H.P., and Bretscher, A. (1989). Disruption of the single tropomyosin gene in yeast results in the disappearance of actin cables from the cytoskeleton. *Cell* 57, 233–242.
- Lorenz, M., Popp, D., and Holmes, K.C. (1993). Refinement of the F-actin model against X-ray fiber diffraction data by the use of a directed mutation algorithm. *J. Mol. Biol.* 234, 826–836.
- Macdonald, F., and Odds, F.C. (1983). Virulence for mice of a proteinase-secreting strain of *Candida albicans* and a proteinase-deficient mutant. *J. Gen. Microbiol.* 129, 431–438.
- Milligan, R.A., Whittaker, M., and Safer, D. (1990). Molecular structure of F-actin and location of surface binding sites. *Nature* 348, 217–221.
- Mösch, H.U., and Fink, G.R. (1997). Dissection of filamentous growth by transposon mutagenesis in *Saccharomyces cerevisiae*. *Genetics* 145, 671–684.
- Mulholland, J., Preuss, D., Moon, A., Wong, A., Drubin, D., and Botstein, D. (1994). Ultrastructure of the yeast actin cytoskeleton and its association with the plasma membrane. *J. Cell Biol.* 125, 381–391.
- Nicholls, A., Sharp, K.A., and Honig, B. (1991). Protein folding and association: insights from the interfacial and thermodynamic properties of hydrocarbons. *Proteins* 11, 281–296.
- Novick, P., and Botstein, D. (1985). Phenotypic analysis of temperature-sensitive yeast actin mutants. *Cell* 40, 405–416.
- Read, E.B., Okamura, H.H., and Drubin, D.G. (1992). Actin- and tubulin-dependent functions during *Saccharomyces cerevisiae* mating projection formation. *Mol. Biol. Cell* 3, 429–444.
- Riezman, H., Munn, A., Geli, M.I., and Hicke, L. (1996). Actin-, myosin- and ubiquitin-dependent endocytosis. *Experientia* 52, 1033–1041.
- Saeki, K., Sutoh, K., and Wakabayashi, T. (1996). Tropomyosin-binding site(s) on the *Dictyostelium* actin surface as identified by site-directed mutagenesis. *Biochemistry* 35, 14465–14472.
- Sandrock, T.M., O'Dell, J.L., and Adams, A.E.M. (1997). Allele-specific suppression by formation of new protein-protein interactions in yeast. *Genetics* 147, 1635–1642.
- Scalettar, B.A., Swedlow, J.R., Sedat, J.W., and Agard, D.A. (1996). Dispersion, aberration and deconvolution in multi-wavelength fluorescence images. *J. Microsc.* 182, 50–60.
- Sikorski, R.S., and Hieter, P. (1989). A system of shuttle vectors and yeast host strains designed for efficient manipulation of DNA in *Saccharomyces cerevisiae*. *Genetics* 122, 19–27.
- Simon, V.R., Swayne, T.C., and Pon, L.A. (1995). Actin-dependent mitochondrial motility in mitotic yeast and cell-free systems, identification of a motor activity on the mitochondrial surface. *J. Cell Biol.* 130, 345–354.
- Sivadan, P., Bauer, F., Aigle, M., and Crouzet, M. (1995). Actin cytoskeleton and budding pattern are altered in the yeast *rvs161* mutant: the Rvs161 protein shares common domains with the brain protein amphiphysin. *Mol. Gen. Genet.* 246, 485–495.
- Smith, M.G., Simon, V.R., O'Sullivan, H., and Pon, L.A. (1995). Organelle-cytoskeletal interactions: actin mutations inhibit meiosis-dependent mitochondrial rearrangement in the budding yeast *Saccharomyces cerevisiae*. *Mol. Biol. Cell* 6, 1381–1396.
- Waddle, J.A., Karpova, T.S., Waterston, R.H., and Cooper, J.A. (1996). Movement of cortical actin patches in yeast. *J. Cell Biol.* 132, 861–870.
- Welch, M.D., Holtzman, D.A., and Drubin, D.G. (1994). The yeast actin cytoskeleton. *Curr. Opin. Cell Biol.* 6, 110–119.
- Wertman, K.F., Drubin, D.G., and Botstein, D. (1992). Systematic mutational analysis of the yeast *ACT1* gene. *Genetics* 132, 337–350.
- Yang, S., Ayscough, K.R., and Drubin, D.G. (1997). A role for the actin cytoskeleton of *Saccharomyces cerevisiae* in bipolar bud-site selection. *J. Cell Biol.* 136, 111–123.
- Zahner, J.E., Harkins, H.A., and Pringle, J.R. (1996). Genetic analysis of the bipolar pattern of bud site selection in the yeast *Saccharomyces cerevisiae*. *Mol. Cell. Biol.* 16, 1857–1870.